Final Draft
of the original manuscript:

Petrenko, V.I.; Avdeev, M.V.; Haramus, V.M.; Bulavin, L.A.; Aksenov, V.L.; Rosta, L.:

Micelle formation in aqueous solutions of dodecylbenzene sulfonic acid studied by small-angle neutron scattering

In: Colloids and Surfaces A (2010) Elsevier

DOI: 10.1016/j.colsurfa.2010.08.023

MICELLE FORMATION IN AQUEOUS SOLUTIONS OF DODECYLBENZENE SULFONIC ACID STUDIED BY SMALL-ANGLE NEUTRON SCATTERING

V.I.Petrenko[1,2], M.V.Avdeev[1], V.M.Garamus[3], L.A.Bulavin[2], V.L.Aksenov[4,1], L.Rosta[5]

[1]Joint Institute for Nuclear Research, Frank Laboratory of Neutron Physics, Dubna, Russia
[2]Kyiv Taras Shevchenko National University, Physics Department, Kyiv, Ukraine
[3]GKSS Research Centre, Geesthacht, Germany
[4]Russian Research Center "Kurchatov Institute", Moscow, Russia
[5]Research Institute for Solid State Physics and Optics, Budapest, Hungary

*CORRESPONDING AUTHOR: Viktor I. Petrenko, Frank Laboratory of Neutron Physics, Joint Institute for Nuclear Research, Joliot-Curie 6, 141980 Dubna, Moscow Reg., Russia. Tel: 007 496 21 64 988. Fax: 007 496 21 65 484. e-mail: vip@nf.jinr.ru.

ABSTRACT.
Structure and interaction parameters of micelles in solutions of dodecylbenzene sulfonic acid (DBSA) in deuterated water are studied by small-angle neutron scattering. The dependences of micellar aggregation number, fractional charge, charge per micelle and surface potential on surfactant concentration are analyzed. A typical increase in the micelle size with the growth in the acid content is found, which can be related to the transition from spherical to rod-like micelles. The obtained data are used for estimating surfactant micelle concentration in water-based ferrofluids stabilized with DBSA.

Keywords: dodecylbenzene sulfonic acid, micelle formation, small-angle neutron scattering, polar ferrofluids

1.Introduction

Dodecylbenzene sulfonic acid (DBSA), $CH_3(CH_2)_{11}C_6H_4SO_3H$, is a popular component of various colloidal solutions. Thus, the doping of the most promising conducting polymer polyaniline [1-5] with functional protonic acids such as DBSA improves its processibility and thermal stability. At the same time DBSA can form micelles, whose presence affects the size of the corresponding polymeric nanoparticles during polymerization. Again, DBSA plays an important role in improving the reaction rate and conversion of esterification for production of organic esters under relatively mild reaction conditions [6]. Also, DBSA is actively used in the double sterical stabilization of

technical water-based ferrofluids [7-11], aqueous dispersions of magnetic (mostly magnetite) nanoparticles. The second surfactant layer at the surface of magnetite in such ferrofluids is formed due to physical adsorption in excess of the acid. So, the micelle formation in these systems is an important factor, which regulates the content of free surfactant molecules in bulk solutions.

Despite the practical use of DBSA, the formation, structure and interaction of its micelles in aqueous solutions are poorly studied. The given work fills the deficiency of information on this question. Small-angle neutron scattering (SANS) is used to find out parameters of the structure and interaction of the DBSA micelles in deuterated water (d-water) as a function of the surfactant concentration in solution. Deuterated water is used to achieve a sufficient scattering contrast between the surfactant and liquid carrier and also for reduction of incoherent scattering background from hydrogen. The structure parameters of the micelles are compared with those obtained [10] for DBSA micelles formed in the above-mentioned water-based ferrofluids. The surfactant content in the bulk of ferrofluids is found.

2.Experimental

First, the critical micelle concentration (*cmc*) of DBSA in water was determined from the surface tension measurements performed with a Krüss Processor Tensiometer K100 using the ring method. Pure DBSA (c.p., Merck) was dissolved in bidistilled water (Millipore) with several volume fractions within the range of 0.001-0.8%. Surface tension was determined at 25 °C by recording ten data points per one concentration within a measuring interval of 300 s.

SANS experiments were performed with the Yellow Submarine small-angle instrument at the steady-state reactor of the Budapest Neutron Centre (BNC), Hungary. The differential cross-section per sample volume (hereafter referred to as scattered intensity) was obtained as a function of the scattering vector module, $q = (4\pi/\lambda)\sin(\theta/2)$, where λ is the incident neutron wavelength and θ is the scattering angle. The fixed wavelength of 0.386 nm (monochromatization $\Delta\lambda/\lambda = 20\%$) and sample-detector distances of 1.3 and 5.6 m (detector size 0.64 m) were used to cover the q-interval of 0.15-4.5 nm^{-1}. SANS measurements were performed at 25 °C. The calibration on 1-mm water sample was made after the background, buffer (D_2O) and empty cuvette corrections in a standard way [12]. Pure DBSA was dissolved in d-water (99.9%, Sigma–Aldrich) within a wide interval of 2-17% in volume fraction.

3.Results and discussion

The experimental values of surface tension $\sigma(\varphi)$ against the logarithm of the concentration (φ, vol. fraction) are plotted in Fig.1. This dependence has a typical shape for micelle formation solutions described well by the expression:

$$\sigma(c) = -A(\ln(cmc)-\ln(c))g(c)+\sigma_o, \quad (1)$$

$$\text{with } g(c)=\begin{cases} 1 \text{ for } c \le cmc \\ 0 \text{ for } c > cmc, \end{cases}$$

where σ_o is the surface tension at surfactant concentrations higher than *cmc* and $A = \partial\sigma/\partial\ln(c)$ (the slope) corresponds to the alteration in the surface tension as a function of the natural logarithm of the surfactant concentration, *c*. The curve in Fig.1 is fitted to the function (1) with the varied *cmc*, σ_o and *A*, which gives *cmc* = $(1.8 \pm 0.01)\cdot10^{-2}$ vol. % = $(5.51 \pm 0.03)\cdot10^{-4}$ M/L, $A = 6.62 \pm 0.02$ mN/m and $\sigma_o = 32.9 \pm 0.1$ mN/m. The obtained value of *cmc* for DBSA is comparable with those for surfactants of the same (C_{12}) alkyl chain length, e.g. sodium p-dodecylbenzene sulfonate (*cmc* = $1.2\cdot10^{-3}$ M/L) or $CH_3(CH_2)_{11}(OCH_2CH_2)_6OH$ (*cmc* = $8.7\cdot10^{-5}$ M/L).

The excess surface concentration Γ can be calculated as [13]:

$$\Gamma = -A/kRT, \quad (2)$$

where *R* is the gas constant, *T* is the temperature. For DBSA as an ionic surfactant the counterions are taken into account by setting $k = 2$ [13]. From the excess surface concentration (Γ) the minimum area per molecule at the air/water interface (S^*) can be found [14]:

$$S^* = (\Gamma\cdot N_A)^{-1}, \quad (3)$$

where N_A is the Avogadro's number. Calculations in accordance with (2), (3) give $\Gamma = 1.34\cdot10^{-6}$ mol/m^2 and $S^* = 1.24$ nm^2.

The obtained experimental SANS curves from micellar solutions are given in Fig.2. They are divided into three groups corresponding conventionally to low ($\varphi < 5\%$), intermediate ($5 \le \varphi < 10\%$) and high ($10\% \le \varphi$) volume fraction of DBSA. The peaks in the experimental SANS curves at $q < 1$ nm^{-1} reflect the interaction between micelles. The position of the interference maximum shifts to a larger *q*-value with an increase in the surfactant concentration, which points to a decrease in the characteristic intermicellar distances in the solution.

Assuming that micelles are monodisperse spheres one can write the scattered intensity in the standard form as:

$$I(q) = n(\Delta\rho)^2V^2F^2(q)S(q), \quad (4)$$

where n is number particle density; $\Delta\rho = \rho - \rho_s$ is the contrast, the difference between the scattering length densities of the particle, ρ, and solvent, ρ_s; V is the micelle volume; $F^2(q)$ is the squared form-factor of a single particle (defined in a way that $F^2(0) = 1$); and $S(q)$ is the structure-factor describing the interaction between micelles. For non-spherical micelles the well-known decoupling approximation [15,16], which assumes that there is no correlation between position and size/orientation of particles can be used, where

$$I(q) = n(\Delta\rho)^2 < \left|F(q)\right|^2 > (1 + \beta(q)[S(q) - 1]). \quad (5)$$

Here, $\beta(q) = \left|< F(q) >\right|^2 / < \left|F(q)\right|^2 >$ is a q-dependent anisotropy factor with <…> denoting the averaging over all possible micelle orientations. To model $S(q)$, we apply the rescaled mean spherical approximation for dilute charged colloidal dispersions developed by Hansen and Hayter [17]. Since the studied micelles consist of ionic surfactant molecules, the screened Coulomb potential is used in the model:

$$U(r) = \pi\varepsilon_0\varepsilon D^2\Psi_0^2 \frac{e^{-(r-D)/k_d}}{r}, \text{ for } r > D, \quad (6)$$

where ε_0 = 8.85·10^{-12} F/m is the vacuum permittivity; ε = 78.5 is the dielectric constant of the solvent medium (water) for 25 °C; D is the particle diameter; $\psi_0 = z/[\varepsilon_0\varepsilon D_0(2 + k_d D_0)]$ is the surface potential, which is related to the charge on the micelle, z; k_d is the usual Debye-Huckel inverse screening length. In addition, the resolution function of the SANS set-up with pin-hole geometry [18] is taken into account when calculating the model curves.

The results of the fits are shown as solid lines in Fig.2. The varied parameters are the aggregation number (N_{agg}), degree of ionization (α), axial ratio (γ) and residual background. They are used for calculating the average size (D_0) and charge (z) of micelles, as well as the inverse screening length (k_d) and surface potential (ψ_0). Both types of the resulting parameters are gathered in Table 1. One can see that the micelle axial ratio grows with the surfactant concentration within the interval of 1.4 - 2.65 thus showing a transition towards elongated (rod-like) particles. This is accompanied by an increase in the mean micelle size. The obtained fractional charge of the micelles (below 0.2) is in agreement with the well-known fact that in micellar systems of ionic surfactants only a fraction of 0.15-0.3 of counterions are dissociated, the rest of them are effectively bound to the micellar surface [19].

A more detailed analysis of the change in the micelle parameters with the DBSA concentration in solution is given in Fig.3. Thus, one can see (Fig.3*a*) that the corresponding

dependence for the aggregation number has two slopes. We associate this observation with the mentioned transition from spherical to rod micelles. For higher surfactant concentrations it is obtained that $N_{agg} \sim \varphi^{0.5}$. This law is usual for micellar systems [20,21]. Again, the expected typical decrease in the charge per micelle and degree of micelle ionization, as well as in the calculated surface potential when increasing the surfactant concentration is observed (Fig.3*b,c,d*). The calculation of the area per molecule on the micelle surface gives about 0.65 nm^2; and it slightly decreases with growing φ. The comparison of this value with the area per molecule at the air/water interface obtained in the surface tension measurements indicates that the surfactant molecules are arranged more closely in the micelles.

For the highest concentration (>0.17 of volume fraction) we observed a significant drop in such a parameter of micelles as the degree of dissociation (charge and surface potential). It can be a real effect as well as a limitation of the decoupling approximation (Eq. 5), there we assume that the position and orientation of micelles are independent. To check this assumption, the structure parameters of micelles (Table 1) are used for estimating the overlapping concentration of DBSA/water solutions (φ^*) (effectively micelles with surfactant length l occupy all the space):

$$\varphi^* \approx \varphi \cdot (V_{\text{sphere\_max}} / V_{\text{sphere\_mean}}) = \varphi \cdot zeta^2 , \qquad (7)$$

where $V_{\text{sphere\_mean}}=4/3\pi l^3 \cdot zeta$ and $V_{\text{sphere\_max}}=4/3\pi(l \cdot zeta)^3$ are the mean and maximum values of micelle volume, respectively. It is obtained that for 17 vol. % of DBSA in water the overlapping concentration is higher than 1 ($\varphi^* = 1.2$), which means that effectively all of the micelles overlap. Thus, the surfactant solutions with higher concentrations cannot be considered in the same way as above with respect to the intermicelle potential, i.e. the decoupling approximation is not valid any more.

Using the obtained SANS curves we can estimate the micelle concentration in the magnetic fluid with magnetite coated by double layer of DBSA formed in excess of free surfactant in the solution [10]. For this purpose we compare these curves with the shape scattering function, $I_c(q)$, which is one of the modified basic functions, introduced and applied recently to the analysis of the contrast variation from ferrofluids of various types [10, 22-28]. In accordance with [22] $I_c(q)$ is the Stuhrmann shape basic function [29] averaged over all particle shapes in the solution. The $I_c(q)$ function obtained from the experimental scattering curves at various contrasts [10] for the discussed ferrofluid (volume fraction of magnetite 1.3% against 2.2% of DBSA) is given in Fig.4, where three scattering levels can be distinguished. The first level ($q < 0.2 nm^{-1}$) shows the presence of fractal aggregates (size > 250 nm), while the second level ($0.2 < q < 0.5 nm^{-1}$) corresponds to primary particles (size ~ 20 nm) composing the aggregates. The third level ($q > 0.5 nm^{-1}$) can be associated

with the micelles of DBSA (size ~5 nm). It is fitted well by the Guinier approximation (Fig.4) with the resulting forward scattering intensity, $I_{mic}(0) = 0.003\times10^{-20}$ cm^3, and the radius of gyration, R_g = 2.0 nm. On the assumption of a spherical shape of the micelles one determines the micelle radius, R = 2.6 nm, in accordance with a well-known relation $R_g^2 = (3/5)R^2$. It is comparable with that for the micelles in pure heavy water obtained in the given work. As the first approximation, where the micelle interaction is neglected, the parameter $I_{mic}(0)$ can be used for estimating the volume fraction, φ_{mic}, of the surfactant in micelles formed in the ferrofluid as follows:

$$I_{mic}(0) = n_{mic}V_{mic}^2 = \varphi_{mic}V_{mic}, \qquad (8)$$

where n_{mic} and V_{mic} are the concentration and volume of the micelles, respectively. The contrast factor is excluded from (8) in accordance with the definition of the shape basic function [29,22]. From (8) we have φ_{mic} = 0.00041. The $I_c(q)$ basic function can also be compared directly with the scattering from micelles in pure d-water. In Fig.4 this is done for the rescaled scattering curve from 2.58% solution of free DBSA. Good consistency can be seen. From the rescaling factor, which takes into account the contrast in the pure micelle solution, we obtain the micelle concentration in the ferrofluid, φ_{mic} = 0.00073, which is higher than the previous estimate. Taking into account CMC (the corresponding volume fraction 0.00018) one obtains the total volume fraction of the non-adsorbed surfactant in the ferrofluid to be 0.00091. This value takes about 5% of the whole surfactant content in the system, with the approximate ratio of 1:4 for the free monomer surfactant and micelles. So, one can conclude that almost 95% of DBSA are effectively adsorbed on the magnetite surface and form the stabilizing shell.

4.Conclusion

To summarize, the micelle formation of DBSA in d-water is detected in SANS experiments. The micelle structure and interaction parameters are obtained as a function of the surfactant concentration in solution. It is shown that DBSA/d-water behaves as a typical solution of ionic surfactants showing the transition from spherical to rod-like micelles with the growth in the surfactant concentration within a range of 2-17 vol.%. The determined dependences can be used in the study of complex systems with DBSA, where potential presence of micelles takes a strong effect on the properties and synthesis of such systems. Particularly, the micelle size is comparable with the size of surfactant aggregates in water-based ferrofluids with double stabilization. Experimental SANS data for aqueous DBSA micelles solutions can be used for estimating the content of the non-adsorbed surfactant in water-based ferrofluids, which is always a question in their structure characterization.

Acknowledgements. The program of JINR-HAS cooperation is acknowledged. The work is partially done in the frame of the project RFBR-Helmholtz (HRJRG-016).

References

1. D. Han, Y. Chu, L. Yang, et al., Reversed micelle polymerization: a new route for the synthesis of DBSAA–polyaniline nanoparticles, Coll. Surf. A 259 (2005) 179-187.
2. S. Shreepathi, R. Holze, Spectroelectrochemistry and preresonance raman spectroscopy of polyaniline-dodecylbenzenesulfonic acid colloidal dispersions, Langmuir 22 (2006) 5196-5204.
3. X. Lu, H.Y. Ng, J. Xu, et al., Electrical conductivity of polyaniline-dodecylbenzene sulphonic acid complex: thermal degradation and its mechanism, Synthetic Metals 128 (2002) 167-178.
4. S.-G. Oh, S.-S. Im, Electroconductive polymer nanoparticles preparation and characterization of PANI and PEDOT nanoparticles, Current Applied Physics 2 (2002) 273-277.
5. X. Lu, C.Y. Tan, J. Xu, et al., Thermal degradation of electrical conductivity of polyacrylic acid doped polyaniline: effect of molecular weight of the dopants, Synthetic Metals 138 (2003) 429-440.
6. Y. Han, Y. Chu, The catalytic properties and mechanism of cyclohexane/DBSAA/water microemulsion system for esterification, J. Mol. Catal. A. 237 (2005) 232-237.
7. D. Bica, L. Vekas, M.V. Avdeev, et al., Sterically stabilized water based magnetic fluids: Synthesis, structure and properties, J. Mag. Mag. Mater. 311 (2007) 17-21.
8. L. Vekas, D. Bica, M.V. Avdeev, Magnetic nanoparticles and concentrated magnetic nanofluids: Synthesis, properties and some applications, China Particuology 5 (2007) 43-49.
9. M.V. Avdeev, V.L. Aksenov, M. Balasoiu, et al., Comparative analysis of the structure of sterically stabilized ferrofluids on polar carriers by small-angle neutron scattering, J. Coll. Inter. Sci. 295 (2006) 100-107.
10. M. Balasoiu, M.V. Avdeev, V.L. Aksenov, et al., Structural organization of water-based ferrofluids with sterical stabilization as revealed by SANS, J. Mag. Mag. Mater. 300 (2006) e225-e228.
11. V.I. Petrenko, V.L. Aksenov, M.V. Avdeev, et al., Analysis of the structure of aqueous ferrofluids by the small-angle neutron scattering method, Physics of the Solid State 52(5) (2010) 974-978.
12. G.D. Wignall, F.S. Bates, Absolute calibration of small-angle neutron scattering data, J. Appl. Cryst. 20 (1987) 28-40.
13. B. Janczuk, A. Zdziennicka, W. Wojcik, The properties of mixtures of two anionic surfactants in water at the water/air interface, Coll. Surf. A 220 (2003) 61-68.
14. R. Zana, Aqueous surfactant-alcohol systems: A review, Adv. Colloid Interface Sci. 57 (1995) 1-64.
15. M. Kotlarchyk, S.H. Chen, Analysis of small angle neutron scattering spectra from polydisperse interacting colloids, J. Chem. Phys. 79 (1983) 2461-2469.

16. J. Kalus, H. Hoffmann, K. Ibel, Small-angle neutron scattering on shear-induced micellar structures, Colloid Polym. Sci. 267 (1989) 818-824.
17. J.P. Hansen, J.B. Hayter, A rescaled MSA structure factor for dilute charged colloidal dispersions, Mol. Phys. 46 (1982) 651-656.
18. J.S. Pedersen, D. Posselt, K. Mortensen, Analytical treatment of the resolution function for small-angle scattering, J. Appl. Cryst. 23 (1990) 321-333.
19. L.A. Bulavin, V.M. Garamus, T.V. Karmazina, et al., Measurements of structural and electrostatis parameters and surface tension of micelles of an ionic surfactant versus concentration, ionic strength of solution and temperature by small-angle neutron scattering, Col. Surf. A 131 (1998) 137-144.
20. M.E. Cates, S.J. Candau, Statics and dynamics of worm-like surfactant micelles, J. Phys.: Condens. Matter 2 (1990) 6869-6892.
21. S. Puvvadat, D. Blankschtein, Thermodynamic description of micellization, phase behavior, and phase separatlon of aqueous solutions of surfactant mixtures, J. Phys. Chem. 96 (1992) 5567-5579.
22. M.V. Avdeev, Contrast variation in small-angle scattering experiments on polydisperse and superparamagnetic systems: basic functions approach, J. Appl. Cryst. 40 (2007) 56-70.
23. A.V. Feoktystov, M.V. Avdeev, V.L. Aksenov, et al., Small-angle neutron scattering contrast variation on magnetite-myristic acid-benzene magnetic fluid, J. Surf. Invest. 3(1) (2009) 1-4.
24. M.V. Avdeev, E. Dubois, G. Mériguet, et al., Small-angle neutron scattering analysis of a water-based magnetic fluid with charge stabilization: contrast variation and scattering of polarized neutrons, J. Appl. Cryst. 42 (2009) 1009-1019.
25. A.V. Feoktystov, M.V. Avdeev, V.L. Aksenov, et al., Contrast variation in small-angle neutron scattering from magnetic fluids stabilized by different mono-carboxylic acids, Solid State Phenomena 152-153 (2009) 186–189.
26. A.V. Feoktystov, L.A. Bulavin, M.V. Avdeev, et al., Small-angle neutron scattering by water-based ferrofluid mixed with polyethylene glycol, Ukr. J. Phys. 54(4) (2009) 348-354.
27. A.V. Feoktystov, L.A. Bulavin, M.V. Avdeev, et al., Small-angle neutron scattering on magnetic fluids stabilized by monocarboxyl acids, Ukr. J. Phys. 54(3) (2009) 266-273.
28. M.V. Avdeev, B. Mucha, K. Lamszus, et al., Structure and in vitro biological testing of water-based ferrofluids stabilized by monocarboxylic acids, Langmuir, accepted (2010).
29. H.B. Stuhrmann, In Modern aspects of small-angle scattering. Ed. Brumberger, H., Kluwer Acad. Publishers, Dordrecht, 1995, pp. 221-254.

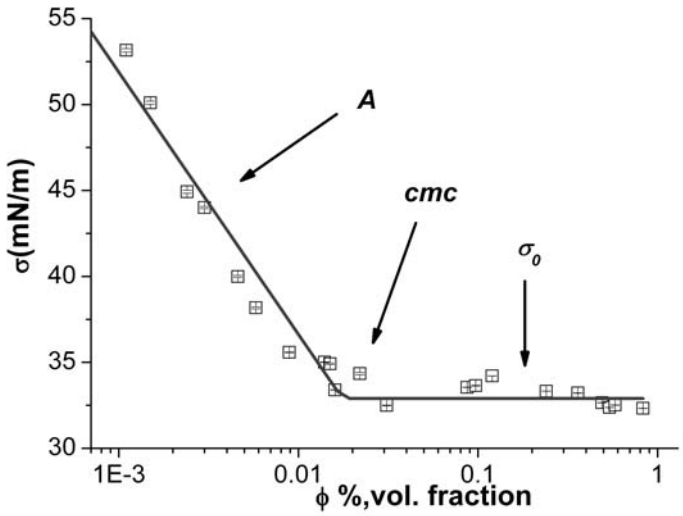

Fig. 1. Determination of the critical micelle concentration by surface tension vs DBSA volume fraction. Solid line shows approximation according to (1).

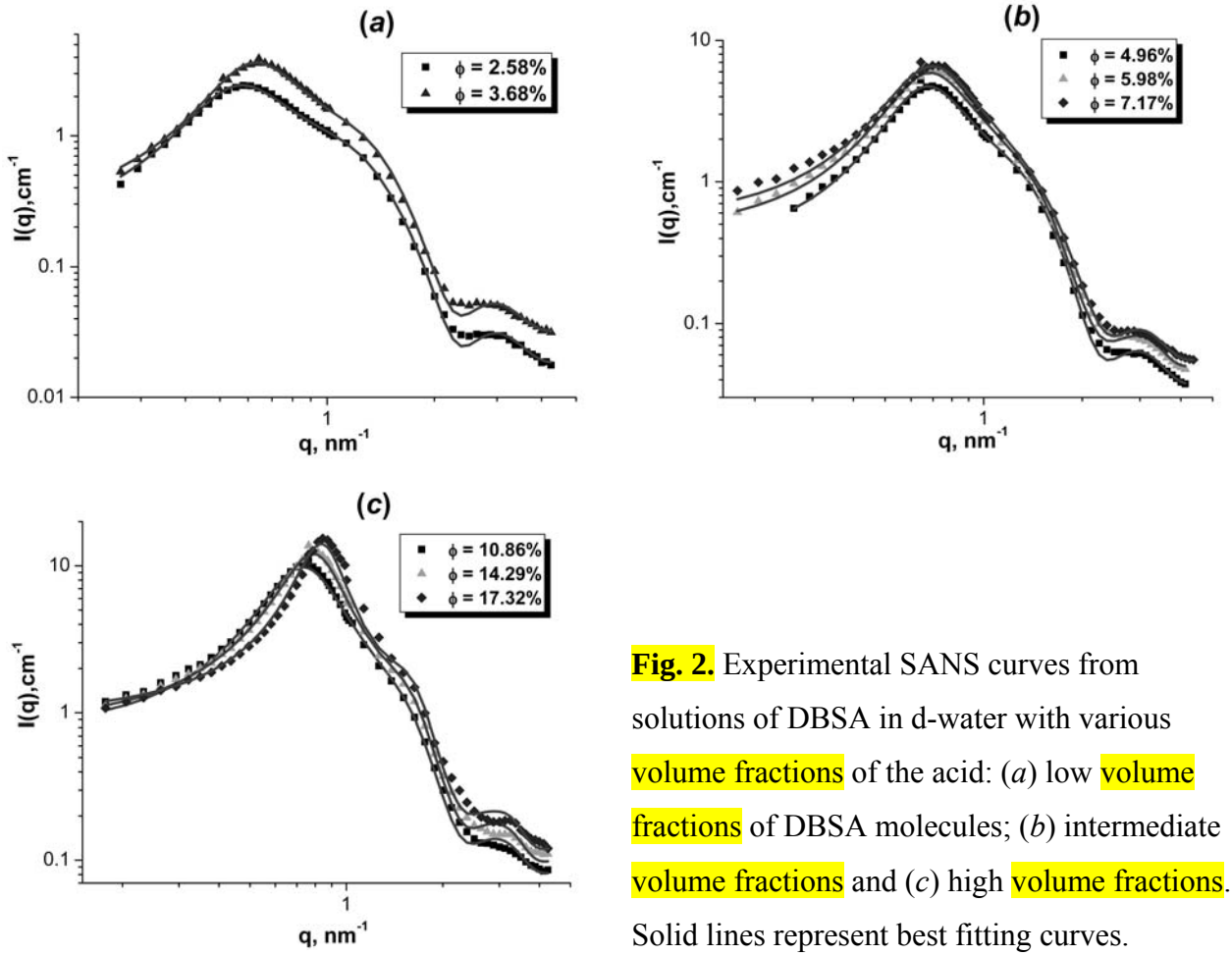

Fig. 2. Experimental SANS curves from solutions of DBSA in d-water with various volume fractions of the acid: (*a*) low volume fractions of DBSA molecules; (*b*) intermediate volume fractions and (*c*) high volume fractions. Solid lines represent best fitting curves.

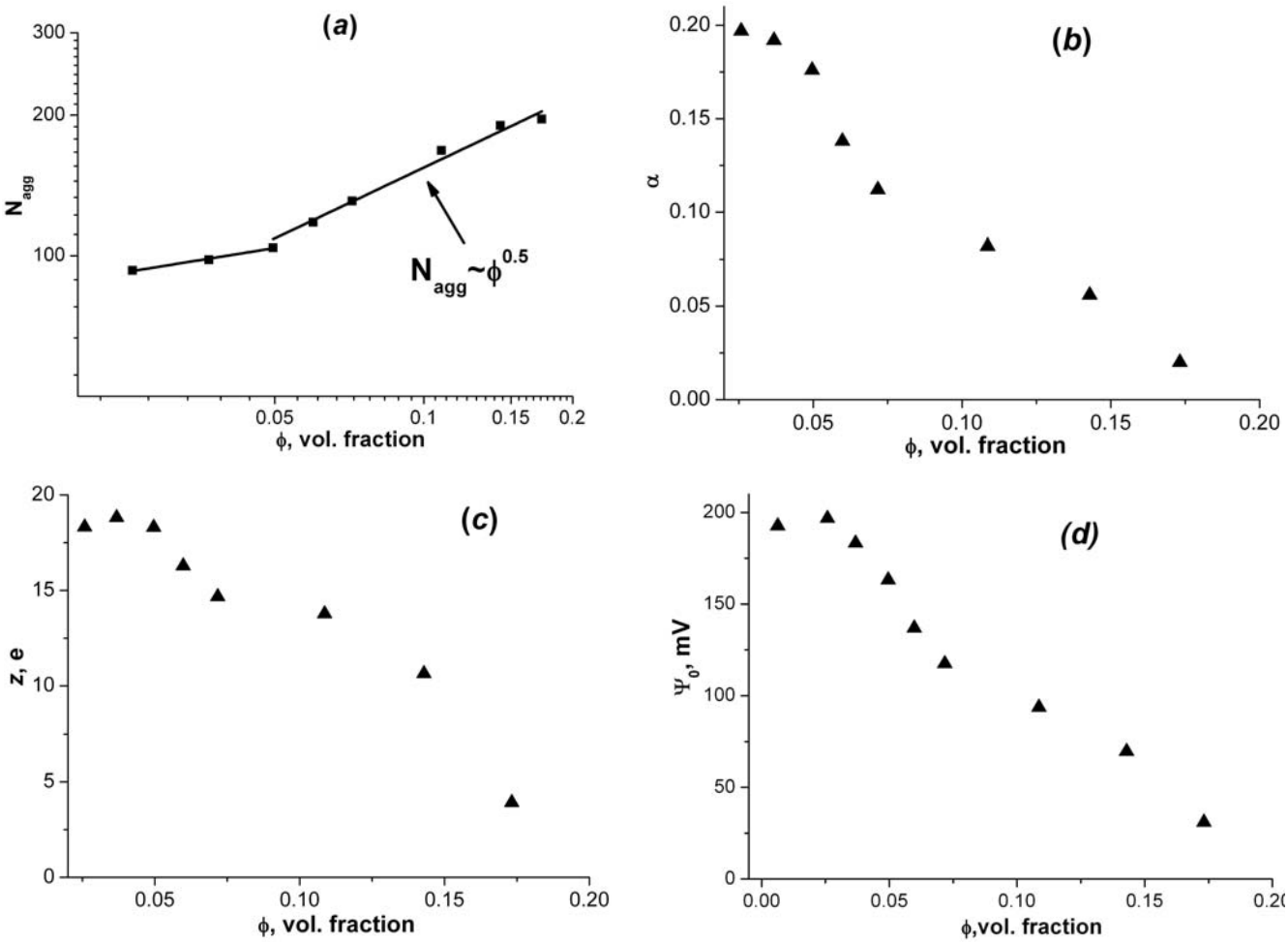

Fig. 3. Dependence of micelle parameters vs. volume fraction of DBSA: aggregation number (*a*), degree of ionization (*b*), charge per micelle (*c*) and surface potential (*d*).

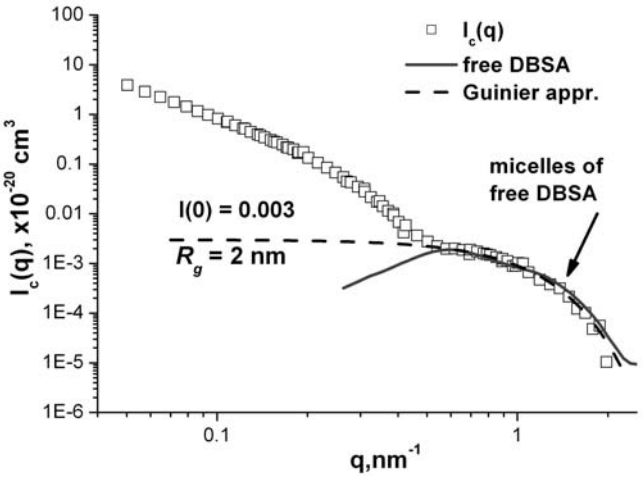

Fig. 4. $I_c(q)$ basic function (points) for water-based ferrofluid stabilized by DBSA is compared with scattering (solid line) from 2.58% solution of free DBSA in D_2O scaled with the proper contrast factor and reduced micelles concentration. Dashed line shows the Guinier approximation to micelle scattering level in $I_c(q)$.

Table 1. Derived from SANS data parameters of DBSA micelles including micelle aggregation number, N_{agg}; degree of ionization, α; axial ratio, γ; average size, D_0; charge, z; inverse screening length, k_d; surface potential, ψ_0.

φ, vol. fraction	N_{agg}	α	γ	**D_0, nm**	**z, e**	**k_d, nm^{-1}**	**Ψ_0, mV**
0.0258	93	0.197	1.4	5.74	18.321	0.3014	197
0.0368	98	0.192	1.4	5.83	18.816	0.3516	183
0.0496	104	0.176	1.49	5.97	18.304	0.3886	163
0.0598	118	0.138	1.64	6.26	16.284	0.3786	137
0.0717	131	0.112	1.91	6.5	14.672	0.3723	117
0.1086	168	0.082	2.33	7.09	13.776	0.3907	94
0.1429	190	0.056	2.58	7.39	10.64	0.3735	70
0.1732	196	0.02	2.65	7.51	3.92	0.2503	31